Denier, James Patrick; Stott, J. A..
The dominant wave mode within a trailing line vortex, *Physics of Fluids*, 2005; 17 (1):14101-1-14101-9.

The dominant wave mode within a trailing line vortex

James P. Denier
School of Mathematical Sciences, The University of Adelaide, Adelaide 5005, Australia

Jillian A. K. Stott
Bradford College, The University of Adelaide, Adelaide 5005, Australia

(Received 4 June 2004; accepted 16 September 2004; published online 23 November 2004)

We identify the dominant, or most unstable, wave mode for the flow in a trailing line vortex. This dominant mode is found to reside in a wavenumber regime between that of inviscid wave modes and the viscous upper branch neutral wave modes. A reevaluation of the growth rate in the vicinity of the upper branch of the curve of neutral stability allows us to predict the neutral value of the azimuthal and axial wavenumber as a function of the imposed swirl within the trailing line vortex. © *2005 American Institute of Physics*. [DOI: 10.1063/1.1814583]

I. INTRODUCTION

We consider the instability of the flow within a trailing line vortex (herein referred to as a TLV). These vortices arise whenever a finite lifting surface terminates in a fluid. The fluid dynamics underlying the generation of these vortices can best be described via Prandtl's lifting line theory, an excellent summary of which can be found in Green.[1]

Trailing line vortices occur in a wide variety of areas in industries ranging from the aeronautical industry, with examples such as the flow over aircraft wings and the rotor blades of helicopters, to the marine industry, with marine propellers, boat keels, and sails being the major examples, through to the energy generation industry with vortices being manifest in the flow over the blades of horizontal and vertical axis wind turbines. In all these areas the generation of TLVs is generally considered undesirable. Perhaps the most important area where TLVs occur and present significant problems is in the aeronautical industry. Here vortex (or lift) induced drag presents a significant problem in terms of the reduced efficiency (and concomitant increased operating costs) of transport aircraft; approximately 35% of the total drag encountered by passenger aircraft is lift induced drag. Given that these vortices persist for a considerable length of time, coupled with the fact that the circulation within the vortex is maximal when the aircraft speed is at its minimum level (that is, during take-off and landing), they pose a significant potential hazard to any following aircraft that may penetrate them (resulting in what is commonly referred to as a wake-vortex interaction). In order to avoid these potentially disastrous encounters aviation authorities throughout the world have prescribed minimum separation distances between successive aircraft during take-off and landing. A detailed discussion of the implications of TLVs to the aviation industry can be found in Ref. 1.

Due to the technological importance of this family of fluid flows the question as to their stability[2] has received considerable attention in the last two decades. There have been two main approaches to the question of flow stability. The first is based upon the numerical solution of the equations governing the growth of infinitesimally small disturbances to the basic, laminar vortex. The second approach revolves around the asymptotic analysis of these equations in a number of physically relevant (and important) limits. In the majority of the work on this problem, the structure of the laminar vortex is taken to be a similarity form derived by Batchelor.[3] This similarity form was derived under the assumption that the distance from the trailing edge of the wing is large. It is therefore of relevance to the flow regime several chord lengths from the trailing edge of the aerofoil. We will exploit this similarity solution as the basic velocity profile for the stability analysis to be presented in this study. To fix ideas in what follows we define a cylindrical coordinate system (r,θ,z) in which z measures the distance downstream of the trailing edge of the lifting surface, rr measures distance radially outwards from the centre of the vortex, and θ measures the azimuthal angle (defined so that θ positive is in the direction of the swirl).

Much of the work on the stability of trailing line vortices has focused on the numerical computation of the growth rates of the instability and in determining the curve of neutral stability in wavenumber-Reynolds number space. The early results of Lessen, Singh, and Paillet[4] demonstrated that the flow is inviscidly unstable to wave modes with azimuthal wavenumber $n \leqslant 1$ over a finite band of axial wavenumbers α. Moreover, the modes with negative azimuthal wavenumber proved to be the most unstable. This work identified the curious behavior that the maximum growth rate of the inviscid wave modes increased with increasing (negative) azimuthal wavenumber n. The value of the axial wavenumber, at which this maximum growth rate occurs, also increases. Thus, this early work presents us with the conclusion that the maximum growth rate corresponds to a short wave (that is, one which has short wavelength in both the axial and azimuthal direction). Lessen and Paillet[5] extended their earlier results to consider the effect of viscosity on the stability of the flow. They solved the cylindrical polar coordinate equivalent of the classical Orr–Sommerfeld equation numerically and were able to determine the parametric curves $F(R_e,\alpha;n,q)=0$ in the Reynolds number (R_e)-wavenumber (α) plane along which the flow is neutrally stable. Such neu-

tral curves have the property that both the upper and lower branches tend to a constant as α becomes large. Subsequent work by Duck and Foster,[6] Khorrami,[7] and Mayer and Powell[8] extended the earlier work of Refs. 4 and 5 and provided a detailed description of the structure of the curve of neutral stability as a function of both the swirl parameter q and the azimuthal wavenumber n. These studies also illustrated that on the inclusion of viscosity (i.e., at finite Reynolds numbers) the most unstable mode occurs for a finite negative value of the azimuthal wavenumber. This effect can be attributed to the interplay between the stabilizing influence of viscosity and the destabilizing effect of swirl.

In-flight Reynolds numbers are large, values in the range $O(10^5)$ to $O(10^6)$ being typical. Considerable progress in understanding the dynamics of the flow can be made by employing an asymptotic analysis based upon the large Reynolds number. Asymptotic theories, valid in the limit of large Reynolds number, were developed (Stewartson,[9] Leibovich and Stewartson,[10] and Duck[11]). These were, in part, driven by earlier numerical results that demonstrated that at large Reynolds number the short wavelength disturbances became concentrated to within a thin layer situated a finite distance from the centerline of the vortex (usually referred to as ring modes). Leibovich and Stewartson[10] derived a sufficient (but not necessary) condition for the existence of *inviscid* modes of instability in a columnar vortex. In the particular case of the Batchelor vortex, for short wavelength disturbances, this condition for instability translates to a restriction on the parameter range given by $\frac{1}{2}nq<\alpha<n/q$ where n and α are the azimuthal and axial disturbance wavenumbers, respectively, and q is a parameter which measures the level of swirl within the flow. Stewartson and Capell[12] considered modes in the vicinity of the upper neutral point ($\alpha\sim n/q$), while Stewartson and Leibovich[13] considered modes close to the lower neutral point ($\alpha\sim nq/2$).

This form of flow structure, exhibiting disturbance localization at a point located within the bulk of the flow, is similar to that reported by Mureithi, Denier, and Stott[14] for the upper branch stability of Tollmien–Schlichting waves in a thermally stratified boundary layer and also to that encountered in the study of centrifugal instabilities in wall bounded flows as described by Denier, Hall, and Seddougui.[15] The results of Ref. 15 provide the impetus for the present study whose motivation is to determine the structure and location of the most unstable wave-like disturbance in a TLV.

To achieve this aim we adopt the following strategy. In Sec. II we formulate the stability problem and derive the large (n,α) asymptotic form for the disturbance field. This is then used in Sec. III to derive the structure of the most unstable disturbance mode in the TLV flow. Finally in Sec. IV we draw some conclusions from our work and comment briefly on some directions for future work.

II. FORMULATION

In order to determine the structure of the most unstable linear disturbance within a trailing line vortex we will proceed in the manner described by Denier, Hall, and Seddougui.[15] In Ref. 15 the wavenumber regime which contains the fastest growing Görtler vortex mode relevant to boundary-layer flows over (concavely) curved surfaces was found. The authors found that consideration of near neutral short wavelength vortices led to the identification of an intermediate regime which contained the most unstable vortex mode. A similar procedure will be adopted in this study.

First we will briefly reconsider the behavior of those wave modes close to the upper branch of the neutral curve; we follow closely the methodology of Stewartson.[9] We will present only those parts of the analysis of Ref. 9 which we consider to be crucial for a clear exposition of the structure of the dominant wave mode. In order to obtain the relevant disturbance equations we write the total nondimensional flow field as the sum of a basic flow plus a small amplitude perturbation

$$(u,v,w,p)=[\overline{u}(r),0,\overline{w}(r),p_0]+\delta[F(r),iG(r),H(r),P(r)/n]E+O(\delta^2), \quad (1)$$

where the velocities (u,v,w) are defined with respect to the cylindrical polar coordinate system (x,r,θ), δ is taken to be infinitesimally small, p is the total pressure, p_0 is the free-stream (constant) pressure, and

$$E=\exp[i\tilde{\alpha}(x-c_0t)+in\theta+ct].$$

Here $\tilde{\alpha}$ is the axial wavenumber, n the azimuthal wavenumber, c_0 denotes the (leading-order) *wave speed*, and c denotes the (complex) growth rate. Substitution of (1) into the Navier–Stokes and continuity equations, in cylindrical polar coordinates, yields at $O(\delta)$,

$$(c+i\phi)F+i\overline{u}'G+\frac{i\tilde{\alpha}}{n}P=\frac{1}{R_e}\left\{\frac{1}{r}(rF')'-\left(\tilde{\alpha}^2+\frac{n^2}{r^2}\right)F\right\}, \quad (2a)$$

$$(c+i\phi)iG-\frac{2\overline{w}H}{r}=-\frac{P'}{n}+\frac{1}{R_e}\left\{\frac{i}{r}(rG')'-\left(\tilde{\alpha}^2+\frac{n^2+1}{r^2}\right)iG-\frac{2inH}{r^2}\right\}, \quad (2b)$$

$$(c+i\phi)H+i\overline{w}^{+}G+\frac{i}{r}P=\frac{1}{R_e}\left\{\frac{1}{r}(rH')'-\left(\tilde{\alpha}^2+\frac{n^2+1}{r^2}\right)H+\frac{2nG}{r^2}\right\}, \quad (2c)$$

$$\tilde{\alpha}F+\frac{n}{r}H=-G'-\frac{G}{r}, \quad (2d)$$

where we have defined

$$\phi=\tilde{\alpha}(\overline{u}-c_0)+\frac{n\overline{w}}{r}$$

and

$$\overline{w}^{+}=\overline{w}'+\overline{w}/r.$$

Here R_e is the Reynolds number of the flow (taken to be large). The basic flow chosen for this study is the similarity

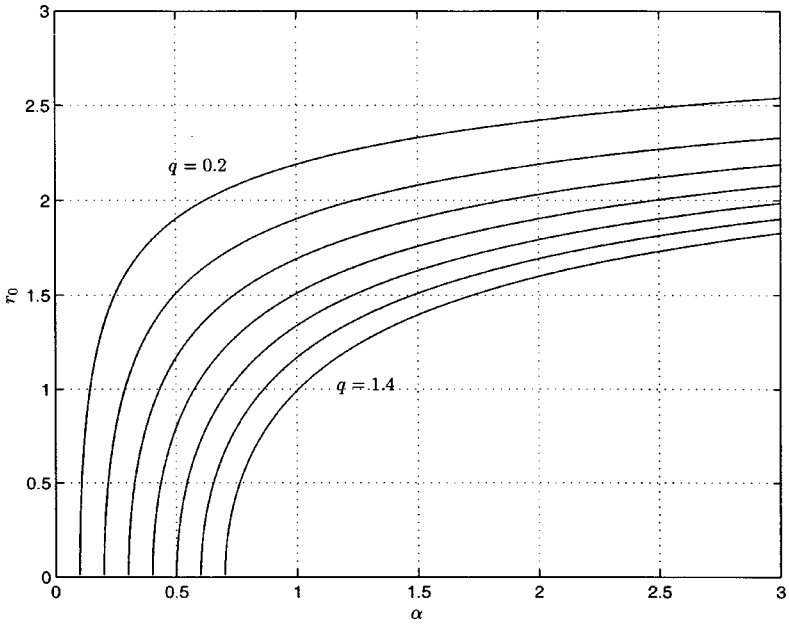

FIG. 1. The radial position r_0 as a function of (scaled) streamwise wavenumber for values of $q=0.2$, 0.4, …, 1.4.

form, first derived by Batchelor,[3] relevant to the flow within a trailing line vortex a distance from the trailing edge of the airfoil. In its simplest form it is given by

$$\overline{u}(r) = e^{-r^2}, \quad \overline{w}(r) = \frac{q}{r}(1 - e^{-r^2}). \tag{3}$$

The parameter q characterizes the intensity of the swirl within the vortex. By making use of (3) for the underlying basic flow we are implicitly assuming that the flow is parallel although, in fact, the velocity field within a TLV does develop spatially. However, the assumption of parallelism is justified in the present case since the wavelengths of the disturbances we will consider are much shorter than the $O(1)$ scales over which the basic flow evolves.

The work of Stewartson[9] demonstrates that the upper branch of the curve of neutral stability is located in the wavenumber regimes $n=O(R_e^{1/2})$, $\tilde{\alpha}=O(R_e^{1/2})$. Thus we write

$$\tilde{\alpha} = \tilde{\alpha}_0 R_e^{1/2}, \quad n = n_0 R_e^{1/2}.$$

Furthermore Ref. 9 shows that, in the vicinity of the upper branch of the neutral curve, the linear disturbances are concentrated in a region of $O(R_e^{-3/8})$ centered on a radial position $r=r_0(\neq 0)$. Thus we define the scaled radial coordinate

$$R = R_e^{3/8}(r - r_0),$$

where the position of the vortex r_0 is to be determined from the subsequent analysis. Within the $O(R_e^{-3/8})$ layer centered on $r=r_0$ the basic flow velocities expand in the form

$$(\overline{u}, \overline{w}) = (\overline{u}_0, \overline{w}_0) + R_e^{-3/8}(\overline{u}_0', \overline{w}_0')R + R_e^{-3/4}(\overline{u}_0'', \overline{w}_0'')R^2 + \cdots,$$

where a prime denotes differentiation with respect to r and a zero subscript will be used to indicate that the function is to be evaluated at $r=r_0$. In addition, the disturbance to the axial velocity expands in the form

$$F = F_0 + R_e^{-1/8}F_1 + R_e^{-1/4}F_2 + \cdots \tag{4}$$

(together with similar expansions for the G, H, and P). We also anticipate the result that the complex growth rate c expands as

$$c = c_1 + R_e^{-1/4}c_2 + \cdots. \tag{5}$$

Substituting these expansions into (2) and equating coefficients of fractional powers of Reynolds number gives, at order $O(R_e^{1/2})$, a system of homogeneous equations for F_0, G_0, H_0, and P_0 which have a nontrivial solution provided that the leading order wave speed c_0 satisfies

$$\tilde{\alpha}_0(\overline{u}_0 - c_0) + \frac{n_0\overline{w}_0}{r_0} = 0, \tag{6}$$

where r_0 is the position at which the disturbance is localized. At next order we again obtain a homogeneous system of equations for the leading-order wave amplitudes which possess nontrivial solutions provided that

$$\tilde{\alpha}_0\overline{u}_0' + n_0\left(\frac{\overline{w}}{r}\right)_0' = 0; \tag{7}$$

this serves to determine the critical location r_0 of the disturbance.

For given values of the azimuthal and axial wavenumbers, n_0 and $\tilde{\alpha}_0$, respectively, r_0 is found from (7) and the leading-order wave speed is determined from (6). From the form of the basic velocity profiles (3) it is readily observed that Eq. (7) possess solutions only for $n_0<0$, assuming q is positive. Conversely if q is negative then solutions to (7) only exist if $n_0>0$; for definiteness we will take q to be positive throughout. In order to highlight this fact we define $\tilde{\alpha}_0=-\alpha n_0$ (and then $\alpha>0$). Equations (6) and (7) can then be rewritten as

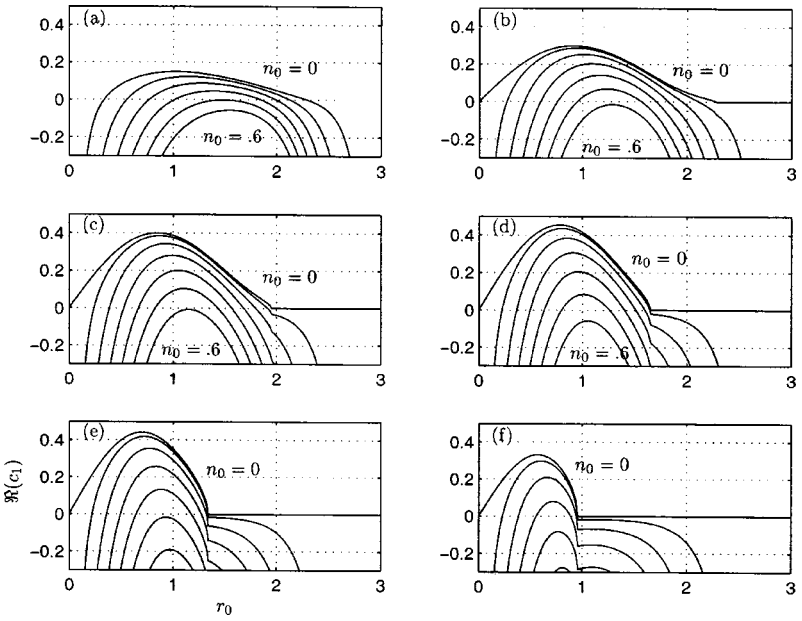

FIG. 2. The real part of the leading-order growth rate as a function of r_0 for various values of swirl parameter (a) $q=0.2$, (b) $q=0.4$, …, (f) $q=1.2$ for $n_0=0.0$, 0.2, …, 0.6.

$$c_0 = \overline{u_0} - \frac{\overline{w_0}}{\alpha r_0}, \quad \alpha = \frac{1}{\overline{u_0'}}\left(\frac{\overline{w}}{r}\right)_0'. \tag{8}$$

In Fig. 1 we present a plot of the critical position as a function of the (scaled) axial wavenumber α for a variety of values of the swirl parameter q. We note that there is a critical value of α (equal to $q/2$) at which the critical position $r_0=0$. As $r_0\to 0$, i.e., in the neighborhood of $\alpha=q/2$, the analysis described in this study breaks down and the wave modes become center modes whose properties have been elucidated by Stewartson and Leibovich.[13] Importantly Fig. 1 clearly demonstrates that the center modes are simply a limiting form of the ring modes which develop as the critical location r_0 approaches the vortex centerline.

Continuing our expansions to next order we obtain

$$\phi_1 F_0 + i\overline{u_0'} G_0 + i\frac{\tilde{\alpha}_0}{n_0} P_0 = 0, \quad i\phi_1 G_0 - \frac{2\overline{w_0}}{r_0} H_0 = 0, \tag{9a}$$

$$\phi_1 H_0 + i\overline{w_0^+} G_0 + \frac{i}{r_0} P_0 = 0, \quad \tilde{\alpha}_0 F_0 + \frac{n_0}{r_0} H_0 = 0, \tag{9b}$$

where we have defined

$$\phi_1 = c_1 + \left(\tilde{\alpha}_0^2 + \frac{n_0^2}{r_0^2}\right), \tag{10}$$

and

$$\overline{w_0^+} = \overline{w_0'} + \overline{w_0}/r_0.$$

This system has a nontrivial solution provided that the determinant of the associated coefficient matrix is identically equal to zero. Evaluating this determinant yields

$$\phi_1 = \pm\left[\frac{2\tilde{\alpha}_0\overline{w_0}(\overline{u_0'} n_0 - \tilde{\alpha}_0 r_0 \overline{w_0^+})}{\tilde{\alpha}_0^2 r_0^2 + n_0^2}\right]^{1/2},$$

which, upon substituting for ϕ_1 from (10), gives the expression for the *leading-order* growth rate,

$$c_1 = \pm\left[\frac{-2\alpha\overline{w_0}(\overline{u_0'} + \alpha r_0 \overline{w_0^+})}{\alpha^2 r_0^2 + 1}\right]^{1/2} - n_0^2\left(\alpha^2 + \frac{1}{r_0^2}\right), \tag{11}$$

where we have made use of our earlier rescaling $\tilde{\alpha}_0=-\alpha n_0$. Note that for the rest of this study we will consider only the positive sign as it is these modes which are unstable. The first term in expression (11) corresponds to the leading-order inviscid growth rate, while the second term is due to the effects of viscosity.

We emphasize here that (11) [and the expression (17) for c_2, to be derived] are as given by Stewartson[9] in his expression (27) with only minor differences in notation. In order to compare his asymptotic results with the earlier numerical results of Lessen and Paillet.[5] Stewartson chose to use these results to construct neutral curves in the (α, R_e) plane for finite values of azimuthal wavenumber n. Although these asymptotic results are derived under the assumption that the azimuthal wavenumber is large and negative, Stewartson found reasonable agreement between computed results and his asymptotic results.

There is, however, an alternative interpretation of the leading-order growth rate which allows us to identify the critical values of the parameters at which the two branches of the neutral curve coalesce. To see this we present, in Fig. 2, plots of the leading-order growth rate $\mathrm{Re}(c_1)$ and in Fig. 3 the first-order correction to the wave speed $\mathrm{Im}(c_1)$ versus r_0 for a variety of values for the swirl parameter q. Three important features are present in Fig. 2. First, for a given value of swirl q there is a critical value of the azimuthal wave number n_0 beyond which the growth rate is negative (for all values of r_0 and hence all values of scaled axial wavenumber α). Second, for values of n_0 below this critical value there are two neutral wave modes. The neutral curves in the (q,α) plane and (q,r_0) plane are presented in Figs. 4 and 5, respectively. For parameter values inside these curves the growth rate c_1 is positive and hence the flow is unstable. As n_0 is increased the level curves in Figs. 4 and 5 shrink until such

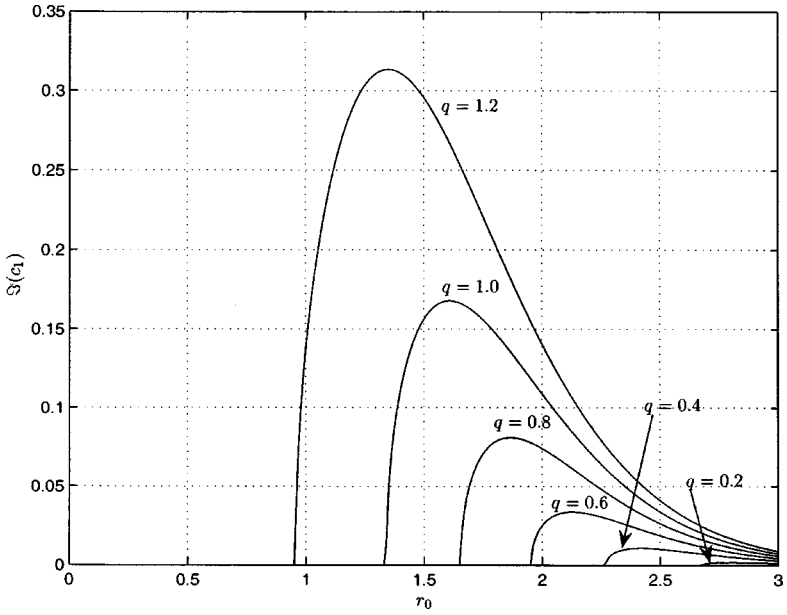

FIG. 3. The imaginary part of the c_1 versus r_0 for values of the swirl parameter $q=0.2, 0.4, \ldots, 1.2$. Note that the imaginary part of c_1 is *independent* of the azimuthal wavenumber n_0.

point that a critical value of n_0 is reached. Beyond this critical value of n_0 the leading-order growth rate c_1 is negative and hence the wave modes described here are stable. In Fig. 6 we present a plot of position r_0 and the corresponding value of swirl q, at which the maximum value of c_1 is identically zero. From this plot the global critical value of n_0 is readily seen. Once this critical value is achieved the curves of neutral stability in the (α, R_e) plane will become closed (at large values of the Reynolds number). The third feature of Fig. 2 that warrants comment is the presence of both center and ring mode instabilities. The ring mode has a position $r_0>0$, the center mode has position $r_0=0$—with the reintroduction of viscosity the center mode [which is neutrally stable with $\mathrm{Re}(c_1)=0$] becomes stabilized $\mathrm{Re}(c_1)<0$.

In Table I we present the critical value of n_0 (and the associated values of q, r_0, and α) together with the limiting numerical results of Mayer and Powell.[8] The agreement between the numerical results of Ref. 8, derived from the numerical solution of (2) for large values of n, and our asymptotic results is excellent.

At this order of approximation the stability of the flow is based upon the sign of c_1; thus, although the results presented in Table I are for the critical value of c_1, the higher order growth rate c_2 [see expression (17)] will modify these critical parameters by an amount of $O(R_e^{-1/4})$. We do not pursue this matter any further here.

To continue, system (9) has the solution

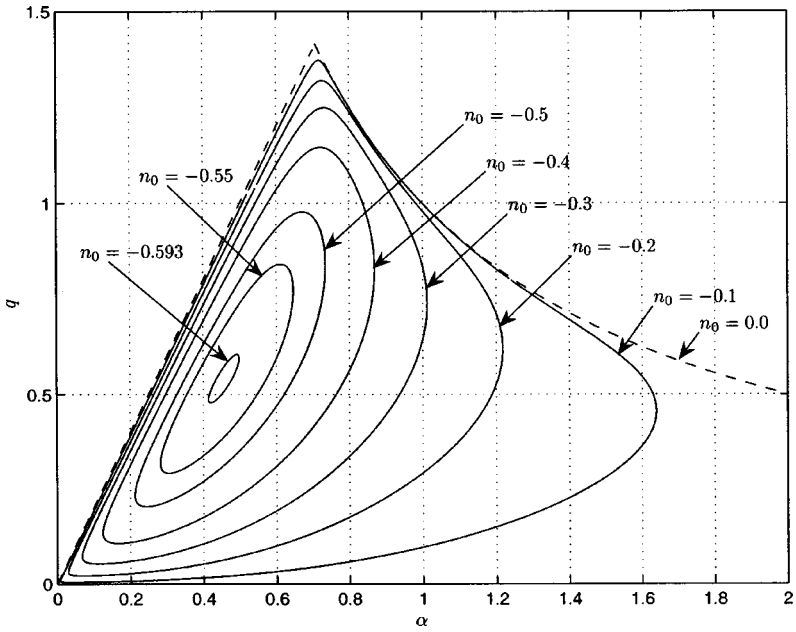

FIG. 4. Neutral curve, based upon the leading order growth rate c_1. Shown are plots of q vs α for various n_0.

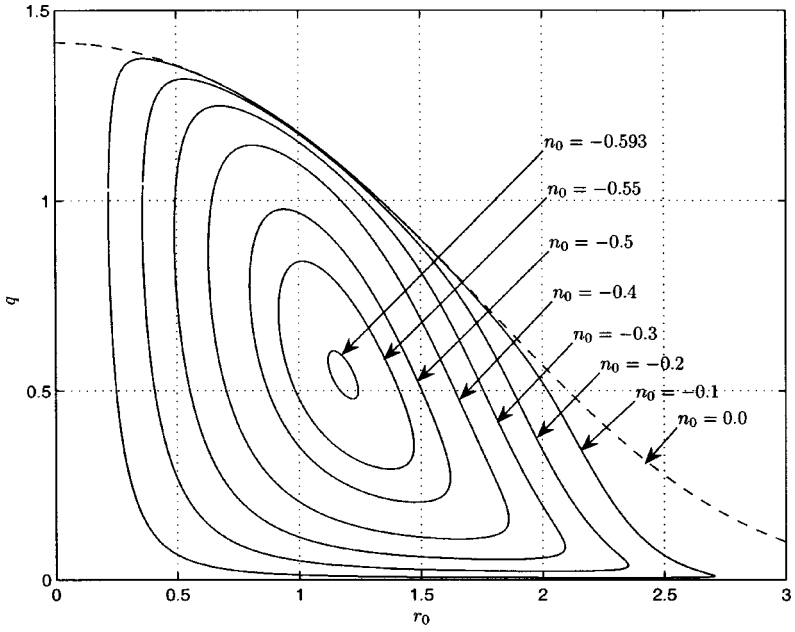

FIG. 5. Neutral curve, based upon the leading order growth rate c_1. Shown are plots of q vs r_0 for various n_0.

$$(H_0, G_0, P_0) = \left(-\frac{\tilde{\alpha}_0 r_0}{n_0}, -\frac{2\tilde{\alpha}_0 \overline{w}_0}{i\phi_1 n_0}, -\frac{n_0}{i\tilde{\alpha}_0}\left[\phi_1 - \frac{2\tilde{\alpha}_0 \overline{u}_0' \overline{w}_0}{\phi_1 n_0} \right] \right) F_0, \tag{12}$$

where the amplitude function F_0 is yet to be determined. At next order in our expansion we obtain the inhomogeneous system of equations for F_1, G_1, H_1, and P_1 which can be solved to give

$$F_1 = -\frac{2i\overline{w}_0 \tilde{\alpha}_0^2 r_0^2}{\phi_1 n_0 (\tilde{\alpha}_0^2 r_0^2 + n_0^2)} \frac{dF_0}{dR} + A_1 F_0, \tag{13a}$$

$$G_1 = \frac{2i\tilde{\alpha}_0 \overline{w}_0 A_1}{\phi_1 n_0} F_0, \tag{13b}$$

$$H_1 = -\frac{2i\tilde{\alpha}_0 r_0 \overline{w}_0}{\phi_1 (\tilde{\alpha}_0^2 r_0^2 + n_0^2)} \frac{dF_0}{dR} - \frac{\tilde{\alpha}_0 r_0}{n_0} + A_1 F_0, \tag{13c}$$

$$P_1 = \frac{2\overline{w}_0 \tilde{\alpha}_0 r_0^2}{(\tilde{\alpha}_0^2 r_0^2 + n_0^2)} \frac{dF_0}{dR} + \frac{n_0}{\tilde{\alpha}_0}\left(\phi_1 - \frac{2\tilde{\alpha}_0 \overline{u}_0' \overline{w}_0}{\phi_1 n_0} \right) i A_1 F_0. \tag{13d}$$

Finally at next order we obtain

$$\phi_1 F_2 + i\overline{u}_0' G_2 + \frac{i\tilde{\alpha}_0}{n_0} P_2 = \mathcal{L} F_0, \tag{14a}$$

$$i\phi_1 G_2 - \frac{2\overline{w}_0}{r_0} H_2 = -\frac{P_1'}{n_0} + i\mathcal{L} G_0, \tag{14b}$$

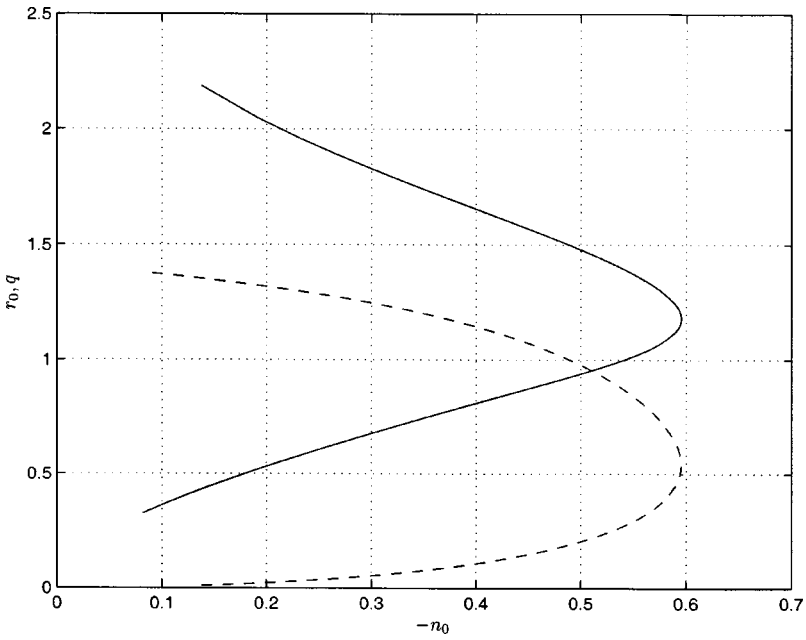

FIG. 6. The position at which the maximum value of c_1 is equal to zero. Shown are r_0 vs n_0 (solid line) and q vs n_0 (dashed line).

TABLE I. The critical values of the azimuthal wavenumber, vortex position, imposed swirl, and axial wavenumber based upon the leading-order growth rate term c_1. The critical Reynolds number is given by $R_{e_0}=1/|n_0|^2$.

	Current study	Mayer and Powell[a]
$\lvert n_0\rvert$	0.595 32	…
r_0	1.181 01	…
q	0.540 55	0.542[b]
α	0.455 50	0.456
R_{e_0}	2.821 6	2.8376

[a]These results are based upon the numerical solution of the stability equations for a value of the azimuthal wavenumber $n=10\,000$ (see their Table IV).
[b]In interpreting the results of Mayer and Powell note that they solved the disturbance equations with n positive and q negative which is equivalent to our case of n negative and q positive.

$$\phi_1 H_2 + i\overline{w_0^+} G_2 + \frac{iP_2}{r_0} = \mathcal{L} H_0, \tag{14c}$$

$$\tilde{\alpha}_0 F_2 + \frac{n_0}{r_0} H_2 = -G_1', \tag{14d}$$

where we have defined the differential operator $\mathcal{L}$

$$\mathcal{L} = \frac{d^2}{dR^2} - c_2 - \frac{in_0\phi_0'' R^2}{2},$$

with

$$\phi_0'' = -\alpha\overline{u_0}'' + \left(\frac{\overline{w}}{r}\right)_0''.$$

System (14) will only have a solution provided that a compatibility condition on the inhomogeneous terms is satisfied. Mathematically this solvability condition is simply the requirement that the inner product of the vector representing the right-hand-side of (14) with the adjoint eigenvector of the coefficient matrix (of the homogeneous system) vanish. Applying this solvability condition, and making use of (13), yields the differential equation governing the radial structure of the wave amplitude F_0,

$$\frac{d^2F_0}{dR^2} - (\lambda_1 R^2 + \lambda_0 c_2) F_0 = 0, \tag{15}$$

where we have defined

$$\lambda_0 = \frac{2(\tilde{\alpha}_0^2 r_0^2 + n_0^2)}{r_0^2 c_1 + 3(\tilde{\alpha}_0^2 r_0^2 + n_0^2)}, \quad \lambda_1 = \frac{i\lambda_0 n_0 \phi_0''}{2}.$$

In order to ensure that the wave mode is confined to the viscous layer centered on $r=r_0$ Eq. (15) must be solved subject to the boundary conditions $F_0\to 0$ as $|R|\to\infty$. Equation (15) is a (modified) form of the parabolic-cylinder-function equation (see Ref. 16) which has the requisite solution if

$$c_2 = -\frac{\lambda_1^{1/2}(1+2m)}{\lambda_0}, \quad m = 0,1,2,\ldots.$$

The corresponding eigenfunctions are given by

$$F_0 = H_m(R)\exp\left(-\frac{1}{2}\lambda_1^{1/2}R^2\right), \tag{16}$$

where H_m are Hermite polynomials of degree m (see Ref. 16 for details).

Again utilizing the scaled axial wavenumber $\alpha=-\tilde{\alpha}_0/n_0$, we obtain (for the first, or $m=0$ mode)

$$c_2 = -\frac{(1+i)\{|\phi_0''|^{1/2}[r_0^2 c_1 + 3n_0^2(\alpha^2 r_0^2+1)]\}^{1/2}}{2(\alpha^2 r_0^2+1)^{1/2}|n_0|^{1/2}}. \tag{17}$$

In deriving (17) we have used the fact that ϕ_0'' is negative for all $r_0>0$ (independent of q). We are now in a position to identify the most unstable wave mode within a trailing line vortex flow.

III. THE MOST UNSTABLE WAVE MODE

To determine the most unstable mode we note from (11) and (17) that, in the limit $n_0\to 0$, we have

$$c_1 \sim \text{const} + O(n_0^2), \quad c_2 \sim O(|n_0|^{-1/2}), \tag{18}$$

where the constant term in (18) is given by

$$\left[\frac{-2\alpha\overline{w_0}(\overline{u_0}' + \alpha r_0 \overline{w_0^+})}{\alpha^2 r_0^2 + 1}\right]^{1/2}.$$

Note that the sign of the term in the square brackets is negative; the constant in c_1 then corresponds to the leading-order growth rate. From (17) we observe that, in the limit of small (scaled) azimuthal wavenumber, the second-order growth rate becomes large, of size $O(|n_0|^{-1/2})$, whereas the correction to c_1 is small, of size $O(n_0^2)$. This suggests that there is a new distinguished limit for n_0 in which these two terms will be of similar size. Noting, from (5), that the correction to the growth rate is $O(R_e^{-1/4}|n_0|^{-1/2})$ we find that the new distinguished limit occurs when

$$n_0^2 = O(R_e^{-1/4}|n_0|^{-1/2}),$$

that is, when $n_0=O(R_e^{-1/10})$ or $n=O(R_e^{2/5})$. Additionally the axial wavenumber $\tilde{\alpha}$ is now of order $O(R_e^{2/5})$. Thus we define

$$n = n_1 R_e^{2/5}, \quad \tilde{\alpha} = \tilde{\alpha}_1 R_e^{2/5}. \tag{19}$$

In order to determine the correct radial scale for the dominant wave mode we observe from Sec. II that in the limit $n_0\to 0$, $\lambda_1\sim O(n_0^3)$ and the eigenfunction is given by (16), or equivalently

$$F_0 = \exp\left[-\tfrac{1}{2}\lambda_1^{1/2}R_e^{3/4}(r-r_0)^2\right].$$

This suggests that the dominant mode is confined to a layer of thickness $O(\lambda^{1/4}R_e^{3/8}) = O(R_e^{3/10})$ centered on the location $r=r_0$. We therefore define

$$\tilde{R} = R_e^{3/10}(r-r_0),$$

and seek wave-like solutions to (2) proportional to

$$E = \exp[i\tilde{\alpha}(x-c_0 t) + in\theta + \hat{c}_1 t + \hat{c}_2 R_e^{-1/5} t],$$

where the amplitude function expands as $F=F_0+R_e^{-1/10}F_1 + R_e^{-1/5}F_2+\ldots$ (with similar expressions for G, H, and P). Substitution of these expansions into (2) gives, at the first

two orders of approximation, the leading-order wave speed and critical position as

$$c_0 = \overline{u}_0 - \frac{\overline{w}_0}{\alpha r_0}, \quad \alpha = \frac{1}{\overline{u}_0'}\left(\frac{\overline{w}}{r}\right)_0', \tag{20}$$

where again α is the ratio of the axial and azimuthal wavenumbers, $\alpha = -\tilde{\alpha}_1/n_1$. This scaled axial wavenumber can be considered to be unchanged from its value in the previous section and correspondingly the functional relationship between the critical position r_0, the wave-speed c_0, and α are as found in Sec. II (see Fig. 1)

Proceeding to the next order in our expansion we obtain the homogeneous system

$$\hat{c}_1 F_0 + i\overline{u}_0' G_0 - i\alpha P_0 = 0, \tag{21a}$$

$$i\hat{c}_1 G_0 - \frac{2\overline{w}_0}{r_0} H_0 = 0, \tag{21b}$$

$$\hat{c}_1 H_0 + i\overline{w}_0' G_0 + \frac{i}{r_0} P_0 = 0, \tag{21c}$$

$$-\alpha F_0 + \frac{1}{r_0} H_0 = 0. \tag{21d}$$

As in Sec. II, system (21) has a nontrivial solution provided that the determinant of the coefficient matrix is identically zero. Evaluating this determinant gives

$$\hat{c}_1 = \left[-\frac{2\alpha\overline{w}_0(\overline{u}_0' + \alpha\overline{w}_0')}{\alpha^2 r_0^2 + 1} \right]^{1/2}, \tag{22}$$

where we have chosen the positive root as it is that which yields unstable modes. This is precisely the leading-order (constant) term which appears in the small n_0 expansion for c_1 from Sec. II; it is *real* and *positive.* At next order, we obtain an inhomogeneous version of (21) which when solved for F_1, G_1, H_1, and P_1 yields

$$F_1 = -\frac{2i\overline{w}_0\alpha^2 r_0^2}{\hat{c}_1 n_1(\alpha^2 r_0^2 + 1)}\frac{dF_0}{d\tilde{R}} + A_1 F_0, G_1 = \frac{2i\alpha\overline{w}_0 A_1}{\hat{c}_1} F_0,$$

$$H_1 = -\frac{2i\alpha r_0\overline{w}_0}{\hat{c}_1 n_1(\alpha^2 r_0^2 + 1)}\frac{dF_0}{d\tilde{R}} - \alpha r_0 A_1 F_0,$$

$$P_1 = \frac{2\overline{w}_0\alpha r_0^2}{n_1(\alpha^2 r_0^2 + 1)}\frac{dF_0}{d\tilde{R}} + \frac{i}{\alpha}\left(\hat{c}_1 - \frac{2\alpha\overline{u}_0'\overline{w}_0}{\hat{c}_1}\right) A_1 F_0.$$

Note that this system yields no information regarding the eigenvalue $\hat{c}_2$. Finally at next order we obtain

$$\hat{c}_1 F_2 + i\overline{u}_0' G_2 + i\alpha P_2 = \mathcal{L} F_0, \tag{23a}$$

$$i\hat{c}_1 G_2 - \frac{2\overline{w}_0}{r_0} H_2 = -\frac{P_1'}{n_1} + i\mathcal{L} G_0, \tag{23b}$$

$$\hat{c}_1 H_2 + i\overline{w}_0' G_2 + \frac{i}{r_0} P_2 = \mathcal{L} H_0, \tag{23c}$$

$$\alpha F_2 + \frac{1}{r_0} H_2 = -\frac{G_1'}{n_1}, \tag{23d}$$

where

$$\mathcal{L} = \frac{d^2}{d\tilde{R}^2} - \hat{c}_2 - \frac{in_1\phi_0''\tilde{R}^2}{2} - n_1^2(\alpha^2 + 1/r_0^2)$$

and ϕ_0'' retains its earlier definition. Applying the solvability (or compatibility) condition to the right-hand side of (23) yields the differential equation

$$\frac{d^2 F_0}{d\tilde{R}^2} - \frac{2n_1^2(\alpha^2 r_0^2 + 1)[(\hat{c}_2 + in_1\phi_0''\tilde{R}^2/2) - n_1^2(\alpha^2 + 1/r_0^2)]}{r_0^2\hat{c}_1} F_0 = 0,$$

which when solved subject to condition that the wave amplitude decays as $\tilde{R} \to |\infty|$ yields the eigenvalue

$$\hat{c}_2 = -\frac{1}{2}\left\{ \frac{i\hat{c}_1 r_0^2 |\phi_0''|^2}{\alpha^2 r_0^2 + 1} \right\}^{1/2} |n_1|^{-1/2} - \frac{|n_1|^2}{r_0^2}(\alpha^2 r_0^2 + 1). \tag{24}$$

From (24) we note that

$$\hat{c}_2 \sim \begin{cases} -|n_1|^{-1/2} & \text{as} \quad n_1 \to 0^- \\ -|n_1|^2 & \text{as} \quad n_1 \to -\infty, \end{cases}$$

and hence $\hat{c}_2$ possesses a global maximum which occurs at

$$n_1 = n_{\max} = -\left[\frac{\hat{c}_1 r_0^6 |\phi_0''|^2}{128(\alpha^2 r_0^2 + 1)^3} \right]^{1/5}. \tag{25}$$

At this point it is useful to briefly summarize the results above. The fastest growing wave mode in the large Reynolds number flow within a trailing line vortex has been identified. It has axial wavenumber $\tilde{\alpha} = -\alpha n_{\max} R_e^{2/5}$, azimuthal wavenumber $n = n_{\max} R_e^{2/5}$ where $n_{\max}$ is given by expression (25). The growth rate is

$$c = \hat{c}_1 + R_e^{-1/5}\mathrm{Re}[\hat{c}_2(n_{\max})], \tag{26}$$

where $\hat{c}_1$ is given by expression (22). From (24) and (25) it can be shown that

$$\mathrm{Re}[\hat{c}_2(n_{\max})] = \gamma\hat{c}_1^{2/5},$$

where γ is a function of r_0, α, and q. Noting that $\hat{c}_1$ is precisely the leading-order *inviscid* growth rate, we have

$$\hat{c}_1 = 0 \text{ when} \begin{cases} \alpha = q/2 & \text{the lower neutral point} \\ \alpha = 1/q & \text{the upper neutral point} \end{cases}$$

(see the $n_0 = 0$ results of Fig. 4 and Ref. 10). Thus in the vicinity of the upper and lower neutral points $\mathrm{Re}[\hat{c}_2(n_{\max})] \to 0$ and the fastest growing mode is, on this basis, stabilized. However, in the limit $\hat{c}_1 \to 0$ the location (in wavenumber space) of the most unstable mode changes. Indeed, from (25) we see that $n_{\max} \to 0$ in this limit and so a new distinguished limit that will arise. We will not explore the details of this additional complication here.

Finally, we emphasize that the analysis presented above is only applicable to the ring modes of instability (i.e., those for which $r_0 > 0$). The most unstable centre mode (with $r_0 = 0$) has yet to be determined.

IV. CONCLUSION

We have derived the values of the critical Reynolds number, azimuthal wavenumber and swirl parameter for short waves within a trailing line vortex, i.e., through the use of a large wavenumber theory we can predict the asymptotically correct value of the swirl parameter beyond which all short wave modes are stabilized. These values provide excellent agreement with the numerical result of Mayer and Powell.[8] Furthermore the most unstable mode for the flow within a trailing line vortex has been described. This mode is found to lie in a wavenumber regime $n = O(R_e^{2/5})$ and $\alpha = O(R_e^{2/5})$. Our description of this most unstable mode corrects the earlier conjecture by Stewartson[9] that the most unstable wave mode has $n = O(R_e^{3/5})$.

What then, is the physical relevance of these short waves and, in particular, the most unstable mode? As noted in the introduction, in-flight Reynolds numbers are typically large and so, in order to accurately model the flow within a TLV we must necessarily develop an understanding of the behavior of disturbances to the flow in the large Reynolds number limit. Here we have identified both the characteristics length scale and structure of the dominant short wave in a typical TLV flow. It is possible to describe a general scenario whereby an otherwise random disturbance to a TLV will grow according to the temporal growth rates of its individual Fourier components. The linear development of such a random disturbance will be dominated by the most unstable mode whose structure has been described in Sec. IV; ultimately, however, this mode will reach an amplitude at which nonlinear terms cannot be ignored and a linear analysis is no longer applicable.

Experimental evidence for the ring modes of instability can be found in Bisgood,[17] Sarpkaya,[18] and Sarpkaya and Daly[19] where the phenomenon of "core bursting" or "core bulging" is discussed. Although it is not possible to obtain any useful information regarding the wavelength of the modes associated with this core bursting it is, as first noted by Khorrami,[7] possible to identify these modes as ring modes (at least in the initial linear stages of their development). The "bursting" results in a spatially localized breakdown of the flow; Sarpkaya[18] demonstrates that this phenomena is different from the classical "vortex breakdown" encountered in closed flows. It is however a nonlinear phenomenon which, as noted above, appears to emanate from the ring modes (that is, a mode that originates a finite distance from the vortex core) which then grow and serve to affect the structure of the flow within the vortex core. The close relationship between the ring modes and the center modes presented here suggest that the nonlinear development of the ring modes may have a role to play in understanding this phenomenon. Now that we have identified the most unstable mode within a TLV flow we are in a position to consider their nonlinear development and thus their effect upon the mean flow component within the TLV. This will be the subject of future work.

ACKNOWLEDGMENTS

This work was supported by the Australian Research Council. The work of J.A.K.S. was undertaken while she was with the Department of Applied Mathematics at the University of Adelaide.

[1] S. I. Green, "Wing tip vortices," in *Fluid Vortices*, edited by S. I. Green (Kluwer, Dordrecht, 1995).
[2] In our discussion of the stability of TLVs we will confine our attention to the question of the stability of a given vortex. The case of the, so called, Crow instability of the counter rotating vortex pair will not be considered.
[3] G. K. Batchelor, "Axial flow in trailing line vortices," J. Fluid Mech. **20**, 645 (1964).
[4] M. Lessen, P. Singh, and F. Paillet, "The stability of a trailing line vortex. Part 1. Inviscid theory," J. Fluid Mech. **63**, 753 (1974).
[5] M. Lessen and F. Paillet, "The stability of a trailing line vortex. Part 2. Viscous theory," J. Fluid Mech. **65**, 769 (1974).
[6] P. W. Duck and M. R. Foster, "The inviscid stability of a trailing line vortex," Z. Angew. Math. Phys. **31**, 524 (1980).
[7] M. Khorrami, "On the viscous modes of instability of a trailing line vortex," J. Fluid Mech. **225**, 524 (1991).
[8] E. W. Mayer and K. G. Powell, "Viscous and inviscid instabilities of a trailing line vortex," J. Fluid Mech. **245**, 91 (1992).
[9] K. Stewartson, "The stability of swirling flows at large Reynolds number when subjected to disturbances with large azimuthal wavenumber," Phys. Fluids **25**, 1953 (1982).
[10] S. Leibovich and K. Stewartson, "A sufficient condition for the instability of columnar vortices," J. Fluid Mech. **126**, 335 (1983).
[11] P. W. Duck, "The inviscid stability of a swirling flow: Large wavenumber disturbance," ZAMP **37**, 340 (1986).
[12] K. Stewartson and K. Capell "On the stability of ring modes in a trailing line vortex: The upper neutral points," J. Fluid Mech. **156**, 369 (1985).
[13] K. Stewartson and S. Leibovich, "On the stability of a columnar vortex to disturbances with large azimuthal wavenumber: The lower neutral points," J. Fluid Mech. **178**, 549 (1987).
[14] E. W. Mureithi, J. P. Denier, and J. A. K. Stott, "The effect of buoyancy on upper branch Tollmien–Schlichting waves," IMA J. Appl. Math. **58**, 19 (1997).
[15] J. P. Denier, P. Hall, and S. O. Seddougui, "On the receptivity problem for Görtler vortices: Vortex motions induced by wall roughness," Philos. Trans. R. Soc. London, Ser. A **335**, 51 (1991).
[16] *Handbook of Mathematical Functions*, edited by M. Abramowitz and I. A. Stegun (Dover, New York, 1965).
[17] P. L. Bisgood, "Some observations of condensation trails," Royal Aircraft Establishment TM FS330 (1980).
[18] T. Sarpkaya, "Trailing vortices in homogeneous and density-stratified media," J. Fluid Mech. **136**, 85 (1983).
[19] T. Sarpkaya and J. J. Daly, "Effect of ambient turbulence of trailing vortices," J. Aircr. **24**, 399 (1987).